

Unbiased estimation of multi-fractal dimensions of finite data sets

A.J. Roberts A. Cronin*

February 1, 1996

Abstract

We present a novel method for determining multi-fractal properties from experimental data. It is based on maximising the likelihood that the given finite data set comes from a particular set of parameters in a multi-parameter family of well known multi-fractals. By comparing characteristic correlations obtained from the original data with those that occur in artificially generated multi-fractals with the *same* number of data points, we expect that predicted multi-fractal properties are unbiased by the finiteness of the experimental data.

Keywords: finite data sets, multi-fractal spectrum, binary multiplicative multi-fractal, generalised dimensions.

1 Introduction

The characterisation of spatial distributions in terms of fractal concepts [7, 3] is becoming increasingly important. In particular, many distributions in nature are found to have the characteristics of a multi-fractal[5, 9]: among many examples are galaxy clustering [1, 8], strange attractors [11], fluid turbulence [12], and plant distributions [2].

*Both at the Department of Mathematics & Computing, University of Southern Queensland, Toowoomba, Queensland 4350, Australia. E-mail: aroberts@usq.edu.au and cronin@usq.edu.au

In application, methods for estimating fractal dimensions are typically unreliable through many problems. Two sources of error lie in largely unknown biases introduced by the finiteness of data sets, addressed by Grassberger [4], and in the finite range of length-scales inherent in gathered data. In many situations where thousands or tens of thousands of data points are known the biases are relatively minor; however, in some interesting problems, for example in the spatial clustering of underwater plants [2], only the order of 100 data points are known and confidence in the fractal results may be misplaced.

We propose to eliminate such biases through a novel method of determining a multi-fractal properties of a given dataset. We compare characteristics of inter-point distances in the data, §2, and in artificially generated multi-fractals. By maximising the likelihood, §3, that the characteristics are the same we may model the multi-fractal nature of the data by the parameters of the artificial multi-fractal. By searching among, §4, artificial multi-fractals with the same number of sample points as in the data, we anticipate that biases due to the finite sample size will be statistically the same in the data and in the artificial multi-fractals, §5; hence predictions should be unbiased. The method also appears to give a reliable indication of the error in the estimates—a very desirable feature as also noted by Judd & Mees [6].

2 Correlation density

Borgani *et al* [1] have surveyed the efficacy of the most popular methods for determining fractal dimensions. They considered: generalised correlation integrals, box counting algorithms, density reconstruction procedures, nearest neighbour methods, and minimal spanning tree methods. Their conclusion is that nearest neighbour and minimal spanning tree methods are inferior. Aesthetically this is pleasing because both of these methods discard much of the available information about inter-point distances that the other methods retain.

Box counting algorithms are very similar to the correlation integrals except that they are non-isotropic. Aesthetically, an isotropic method is preferred and so here we ignore box counting methods.

Borgani *et al* also conclude that correlation integrals are most reliable for generalised dimensions, D_q , of positive order, $q > 0$, and less reliable for

negative order. In contrast, they maintain that the density reconstruction procedure is more reliable for negative order, $q < 0$, and less so for positive order. The same conclusions are also reached by Martínez [8]. Interestingly, both approaches are based on the same processed data; they just fit straight lines in complementary manners.

Given a finite set of N data points \vec{x}_i sampled from some spatial distribution, define the correlation functions $C_i(r)$ as the fraction of points within a distance r of the i th data point. Then the partition function

$$Z(r, q) = \frac{1}{N} \sum_{i=1}^N C_i(r)^{q-1}, \quad (1)$$

is expected to scale as r^τ over the range of length-scales on which the multifractal properties hold. By fitting such a power law to $Z(r, q)$, the generalised dimension D_q is then found from

$$\tau = (q - 1)D_q. \quad (2)$$

For example, the Hausdorff dimension is estimated with $q = 0$, the correlation dimension with $q = 2$, and the information dimension with $q \rightarrow 1$.

Conversely, the density reconstruction method is based on $R_i(c)$ which is the radius of the smallest ball centred on the i th point that contains a fraction c of the data points. Then the partition function

$$W(c, \tau) = \frac{1}{N} \sum_{i=1}^N R_i(c)^{-\tau}, \quad (3)$$

is expected to scale as c^{1-q} over a respectable range of fractions c . Then by fitting a power law, D_q may be again estimated from (2).

At the heart of both of these methods are the curves $C_i(r)$ and $R_i(c)$ which are precisely the inverse function of each other. Imagine plotting all of the curves, $i = 1, \dots, N$, in the rc -plane, and observe that:

- the correlation integral $Z(r, q)$ is just an average of these curves over c at fixed r ;
- whereas in the density reconstruction $W(c, \tau)$ is an average of the curves over r at fixed c .

One method is reputedly good for positive q , the other for negative q . Perhaps by using the data in the rc -plane directly, we can avoid such a dichotomy between positive and negative q .

We propose to base our method on the correlation density, $p(r, c)$, defined as being proportional to the number of $C_i(r)$ curves (or equivalently the $R_i(c)$ curves) which pass near the point (r, c) . In practise we divide the $\log r, \log c$ -plane into rectangular bins of width Δr and Δc , and compute $p_{jk} = p(r_j, c_k)$ as the fraction of curves with $\log c_k - \Delta c/2 < \log C_i(r_j) < \log c_k + \Delta c/2$. See Figure 1 for example.

To emphasise that the previous two good methods are both based on this same picture, observe that to $\mathcal{O}(\Delta^2)$:

$$Z(r_k, q) = \sum_j p_{jk} c_j^{q-1}, \quad (4)$$

whereas

$$W(c_j, \tau) = \sum_k p_{jk} r_k^{-\tau}. \quad (5)$$

3 Maximum likelihood multi-fractal

The task now is to fit the correlation density $p(r, c)$ in a manner so that subsequently we deduce a multi-fractal spectrum for the original data. Our idea is to determine parameters of a multiplicative multi-fractal which best fits the correlation density of the original data. Then our estimate of the multi-fractal spectrum of the data is that of the multiplicative multi-fractal.

The best fit is determined by:

- generating N points on a random multiplicative multi-fractals with a given set of parameters;
- constructing its correlation density $P_{jk} = P(r_j, c_k)$ on the same grid in the rc -plane as used in approximating $p(r, c)$ for the original data;
- estimating the likelihood that the two densities, p and P , come from the same distribution;
- and seeking to alter the parameters of the multiplicative multi-fractal in order to maximise this likelihood.

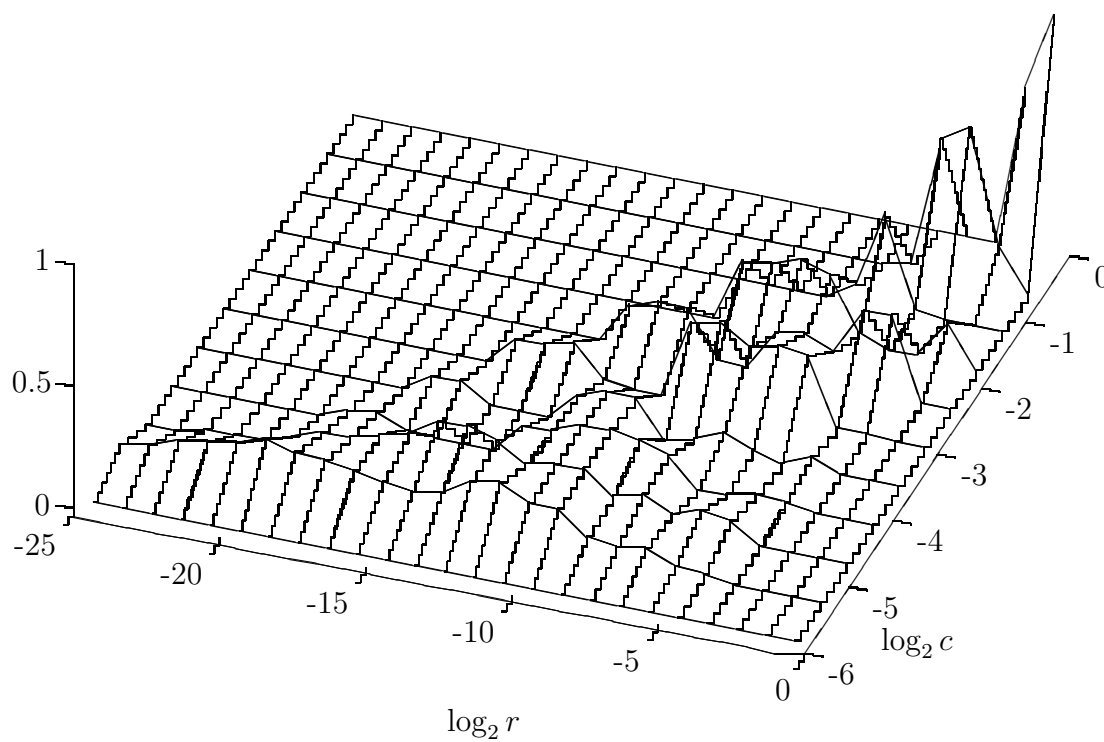


Figure 1: perspective view of the correlation density $p(r, c)$, as a function of $\log r$ and $\log c$, for a sample of $N = 100$ points from the artificially generated binary multiplicative multi-fractal shown in Figure 2 with parameters $\rho = 1/3$, $\phi = 1/4$.

By probing the structure of the N data points by artificially generated fractals with precisely the same number of points we hope to eliminate, or at least reduce, biases introduced by the finiteness of the sample size.

For definiteness, consider a sample of N data points x_i from a multi-fractal on the interval $[0, 1]$ in one-dimension.

We fit from a two parameter family of binary multiplicative multi-fractals. Given parameters $\rho \in [0, 0.5]$ and $\phi \in [0, 0.5]$ a binary multiplicative multi-fractal is generated by the recursive procedure of dividing each interval into two halves, then assigning a fraction ϕ of the points in the interval to a random sub-interval of length ρ in the left half, and the complementary fraction $\phi' = 1 - \phi$ to a random sub-interval of length ρ in the right half. See, for example, the distribution shown in Figure 2. Such a binary multiplicative multi-fractal has spectrum $f(\alpha)$ [5, §4] given parameterically in terms of $0 < \xi < 1$ and $\xi' = 1 - \xi$ as

$$f = \frac{\xi \log \xi + \xi' \log \xi'}{\log \rho}, \quad \alpha = \frac{\xi \log \phi + \xi' \log \phi'}{\log \rho}. \quad (6)$$

Other multi-fractal properties, such as generalised dimensions, then also follow, for example, the Hausdorff dimension is just $D_0 = \log 2 / \log(1/\rho)$.

The likelihood that two correlation densities come from the same distribution is determined from the χ^2 statistic [10, §14.3]

$$\chi^2 = \sum_{p_{jk} + P_{jk} > 0} \frac{(p_{jk} - P_{jk})^2}{p_{jk} + P_{jk}}. \quad (7)$$

Since the likelihood is monotonic in χ^2 (for fixed number of degrees of freedom), maximising likelihood is equivalent to minimising χ^2 . Of course there are correlations in the structure of the correlation densities $p(r, c)$; for example, the $C_i(r)$ curves are monotonic. Strictly speaking these correlations destroy the precise applicability of the likelihood and the χ^2 statistic. However, as is typical in estimating fractal properties, such correlations are intrinsic to investigating structures over many different length scales and are not expected to have a serious effect.

4 Optimum fit

We then seek to find values of ρ and ϕ such that the χ^2 comparison between the actual data and the artificially generated data is minimum. Unfortu-

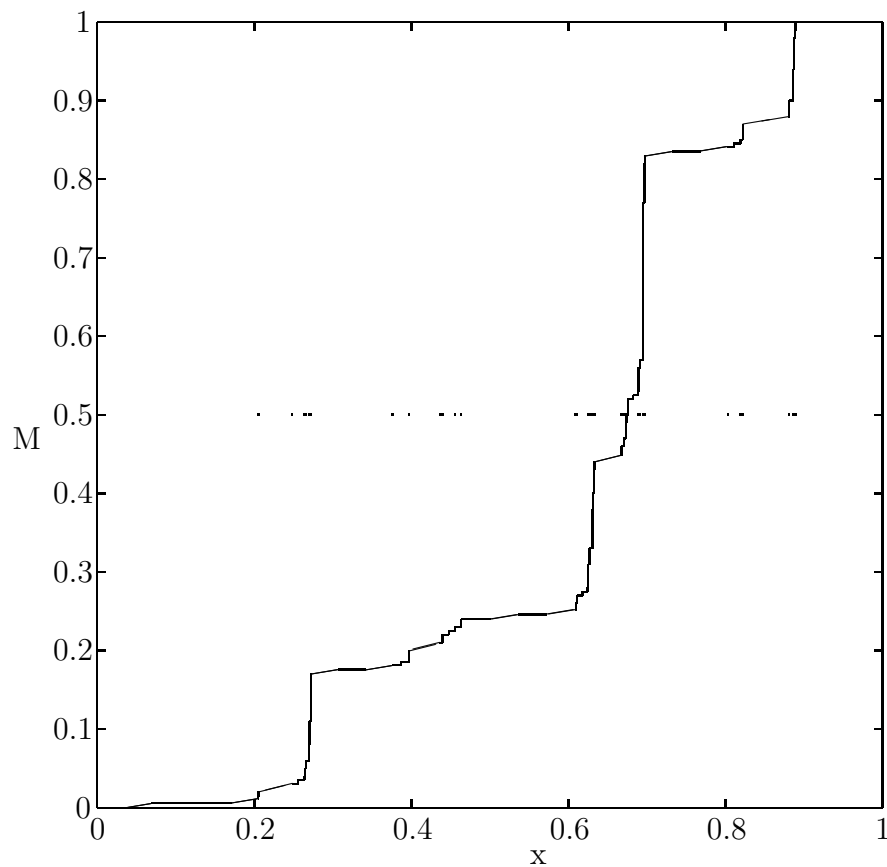


Figure 2: across the middle of this graph is plotted $N = 100$ points on an artificially generated binary multiplicative multi-fractal with parameters $\rho = 1/3$ and $\phi = 1/4$. The solid line is the cumulative mass distribution on the fractal, $M(x) = \text{mass in } [0, x]$, showing regions of high density by large jumps in M .

nately, $\chi^2(\rho, \phi)$ has a large amount of noise due to the random choices in the generation of the artificial binary multiplicative multi-fractals. Such randomness is absolutely necessary because it characterises the wide range of possible multi-fractals with the same multi-fractal spectrum. (It would only be possible to eliminate the noise if we knew a precise analytic expression for the correlation density $P(r, c)$ for a binary multiplicative multi-fractal with parameters ρ and ϕ and when sampled by N points.) As is reasonable, the noise in $\chi^2(\rho, \phi)$ seems to be particularly prominent for small sample sizes N .

The practical task is to minimise a noisy function of ρ and ϕ . Various approaches were tried; however, a crude procedure reminiscent of simulated annealing seems to be effective. We choose the m parameters (ρ_ℓ, ϕ_ℓ) , typically $m = 100$, of least evaluated χ^2 from a sample of parameter values. The sample of parameter values is initially uniformly randomly distributed over parameter space, $[0, 0.5] \times [0, 0.5]$, and then more are generated from the m most successful so far. Typically 20 iterations were performed, constructing some 2000 artificial multi-fractals and using χ^2 to compare their correlation density with the original. Ultimately we end with a cloud of m points, as shown in Figure 3, corresponding to parameters which have realised multi-fractals with a good fit to the correlation density of the original data. The centre of the cloud, the mean of the parameter points, is our best estimate of the appropriate parameters to use in order to model the original data. The spread of the cloud is indicative of the sensitivity of the parameter estimation to the noise inherent in fitting to the correlation density given the limited amount of information in N data points—the spread depends upon the signal:noise ratio.

The optimisation procedure reminds us of simulated annealing in that parameter values are retained depending upon randomness, though here the randomness is intrinsic to the function rather than externally imposed. The “temperature”, which is progressively lowered in simulated annealing, is analogous to the threshold of the m th best parameter value, which decreases from one iteration to the next.

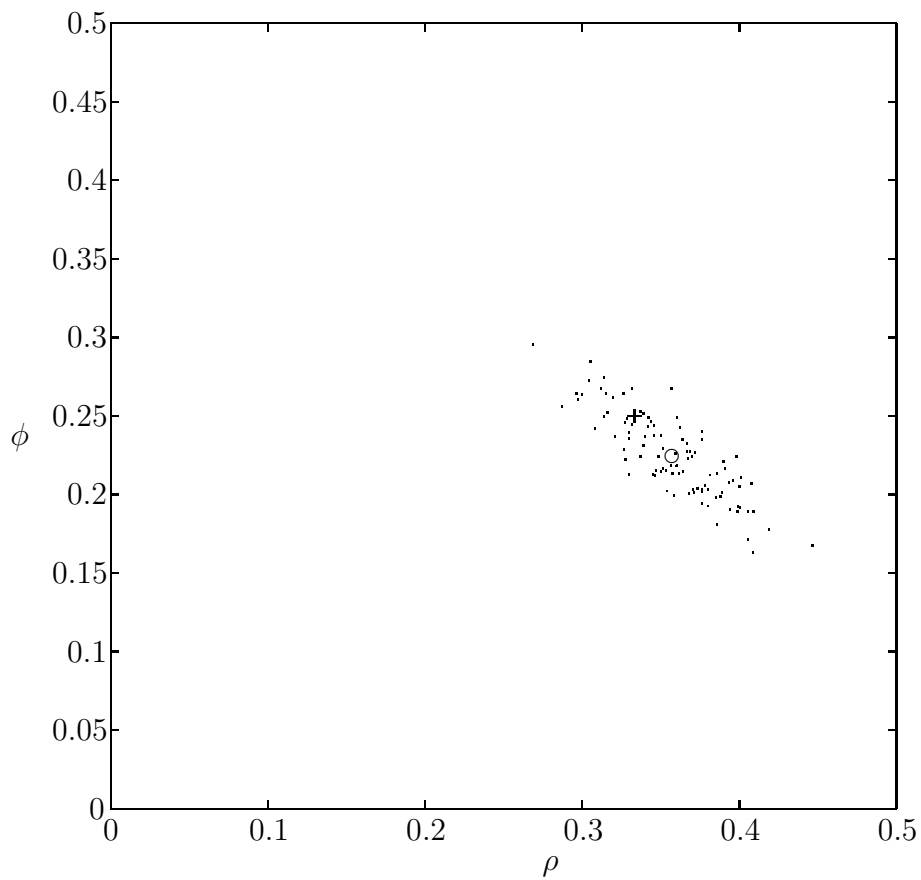


Figure 3: a cloud of $m = 100$ parameter values which match to a good degree of likelihood with an artificially generated binary multiplicative multi-fractal with parameters $\rho = 1/3$ and $\phi_1 = 1/4$. The + denotes the actual parameters used to generate the original data sample, whereas the o denotes the mean of the the cloud as our best estimate of the parameters.

5 Numerical experiments

One numerical trial consists of generating a multiplicative multi-fractal with a specific value of its parameters, here we chose $\rho = 1/3$ and $\phi = 1/4$ throughout, sampled with N points where here we used $N = 30, 100$ (shown previously) or 300. This multi-fractal forms the synthetic finite data set. Then the above procedure is applied and the mean of the ultimate cloud of parameter values recorded as an estimate of the parameters of the synthetic data.

To test the method, we performed 16 different trials with $N = 30$ data points, $N = 100$, and $N = 300$. The estimates of the multi-fractal parameters for $N = 100$ and $N = 300$ are shown in Figures 4 and 5, respectively. Observe that, as would be expected, the parameter predictions improve for the larger value of N . Also observe that the numerical predictions of (ρ, ϕ) are reasonably centred upon the true values of $(1/3, 1/4)$. The method does indeed seem to lack any bias due to the finite size of the sample.

Going to an extremely small number of data points, $N = 30$, as shown in Figure 6 we find that apart from two bad realisations (of small ρ , high ϕ) the predicted multi-fractal parameters are semi-quantitative in that they indicate a reasonably limited area of the parameter space in which the actual multi-fractal parameters are to be found. We consider this an impressive result for such a small N .

A useful observation is that the spread observed between the estimates in such an ensemble of realisations, such as in Figure 4, is approximately the spread observed in the cloud of high likelihood parameters, see a corresponding cloud in Figure 3: the covariances are very similar. The similar spread of the cloud of high likelihood comparisons to the inherent error of the multi-fractal parameter prediction is also demonstrated in Figures 6 and 5 where the cloud for just one of the realisations is also plotted. Thus in application, where one generally cannot undertake more than one sample, we expect that the cloud will be a reliable estimate of the region within which we can confidentially expect the true multi-fractal parameters to lie. Indeed, it was almost always the case that the true value of (ρ, ϕ) lay within the cloud of high likelihood parameter values (the only exceptions being the two bad fits with $N = 30$ data points). Thus the covariance matrix of the cloud gives a good indication of the error in the fitted parameter values.

We expect that the reason the cloud gives a good estimate of the error is

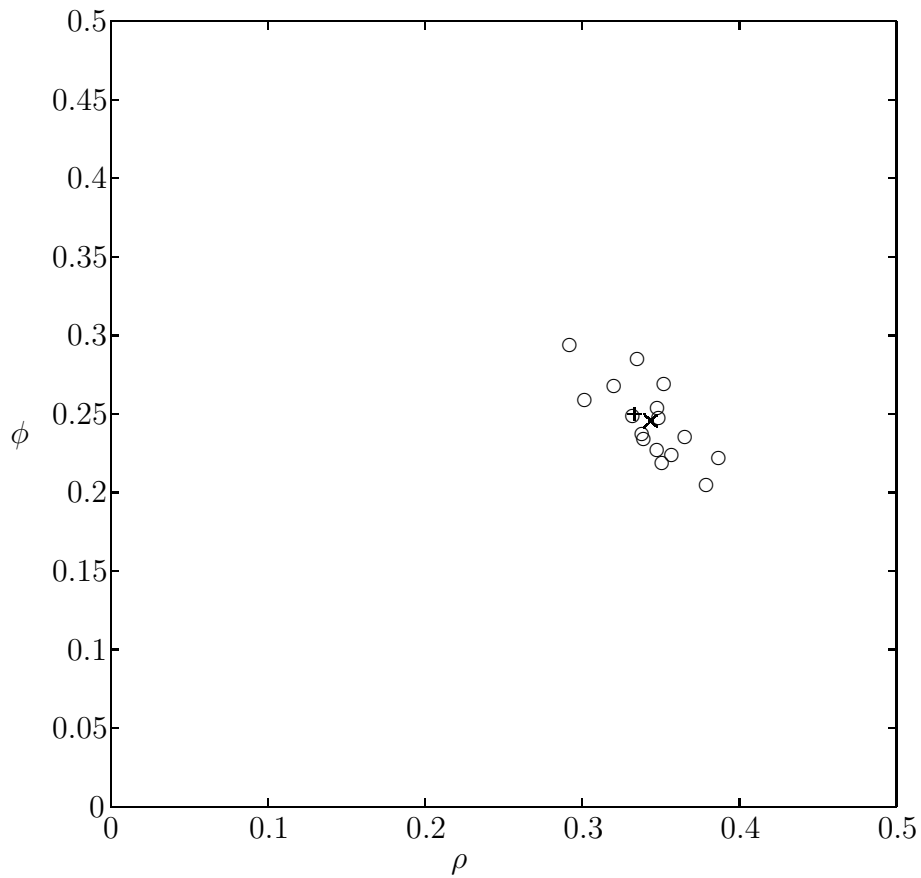


Figure 4: predicted multi-fractal parameters (ρ, ϕ) , indicated by \circ 's, from the maximum likelihood match to an ensemble of 16 different realisations, each of $N = 100$ data points, of a binary multiplicative multi-fractal with parameters $\rho = 1/3$ and $\phi = 1/4$, indicated by $+$. The mean location of the realisations and predictions is indicated by a \times .

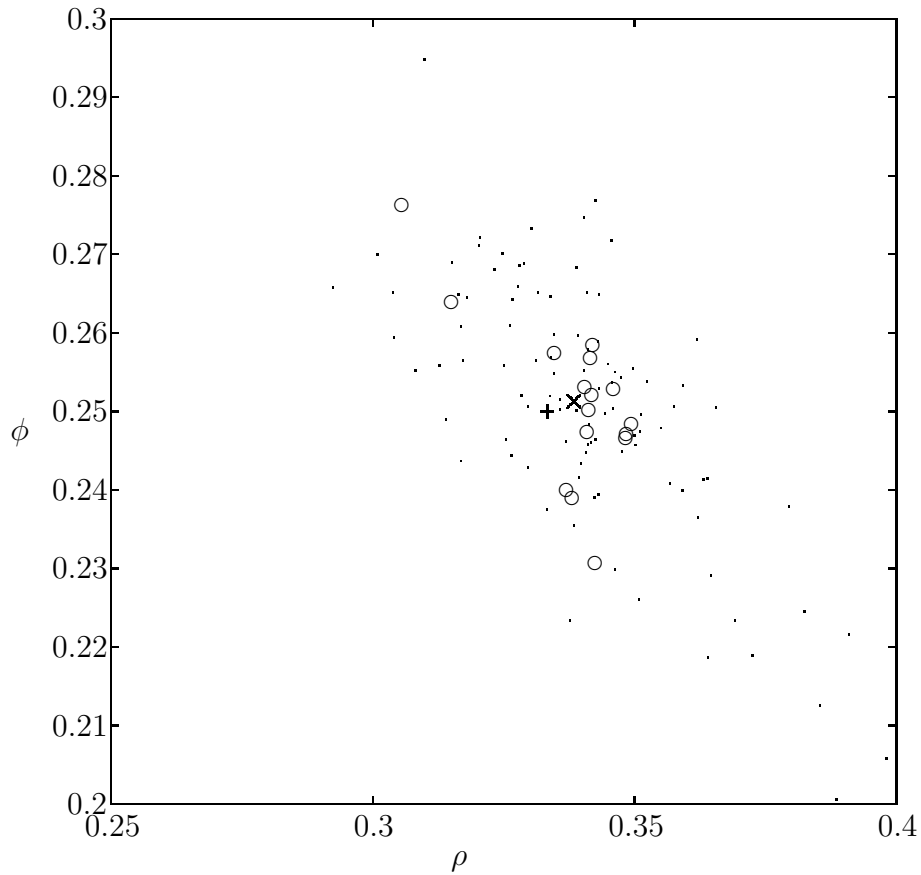


Figure 5: predicted multi-fractal parameters (ρ, ϕ) , indicated by o's, from the maximum likelihood match to an ensemble of 16 different realisations, each of $N = 300$ data points, of a binary multiplicative multi-fractal with parameters $\rho = 1/3$ and $\phi = 1/4$, indicated by +. The mean location of the realisations and predictions is indicated by a \times . A cloud of best likelihood comparisons for one of the realisations is shown by the dots. Note the change in scale for this Figure.

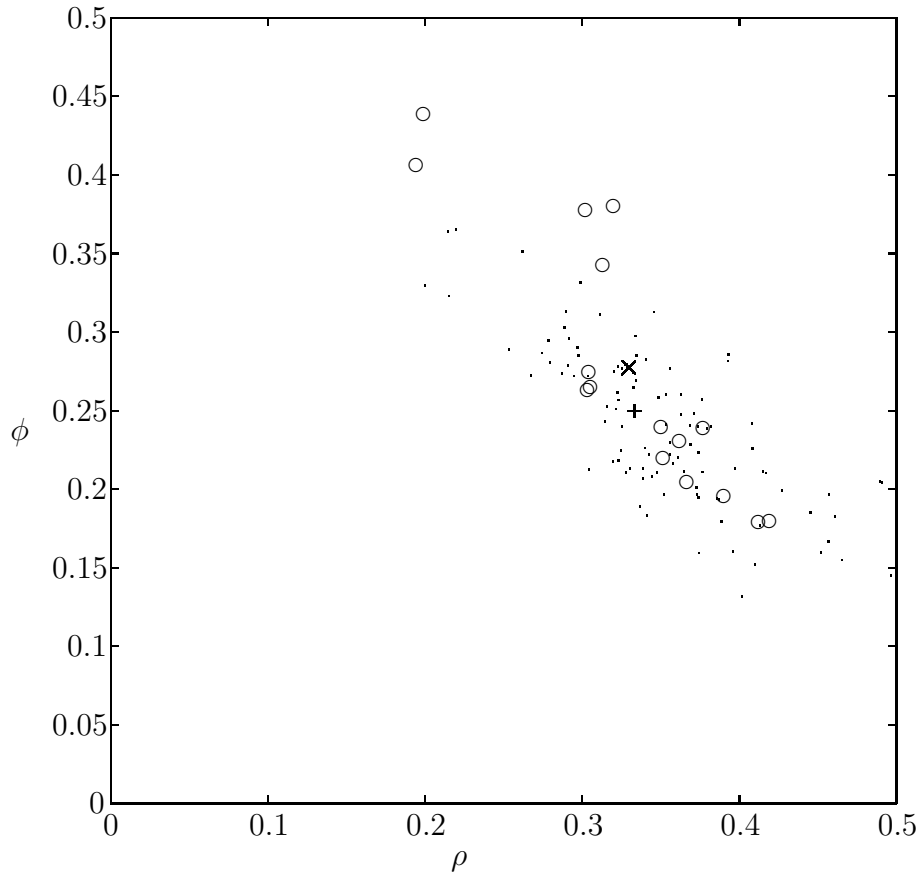


Figure 6: predicted multi-fractal parameters (ρ, ϕ) , indicated by \circ 's, from the maximum likelihood match to an ensemble of 16 different realisations, each of $N = 30$ data points, of a binary multiplicative multi-fractal with parameters $\rho = 1/3$ and $\phi = 1/4$, indicated by $+$. The mean location of the realisations and predictions is indicated by a \times . A cloud of best likelihood comparisons for one of the realisations is shown by the dots.

that the size of the cloud is characteristic of the signal:noise ratio in $\chi^2(\rho, \phi)$. However, the noise comes from randomly sampling a multi-fractal, namely the binary multiplicative multi-fractal, and hence is similar to the bias introduced by the *same* sized sample of the natural process that generated the original data. Thus the influence of this bias is characteristic of the influence of the noise we see in the analysis, and so the latter may be used to predict errors.

Ultimately, researchers want to examine multi-fractal properties of the data. In this method these will be determined from the parameters of the best fit multi-fractal. For example, for any determined parameters (ρ, χ) for the binary multiplicative multi-fractal, the multi-fractal spectrum of the data it matches would be predicted to be given by the analytic expression (6). For the 16 realisations of the $N = 100$ data-point multi-fractals, we determined various estimates, plotted by \circ 's in Figure 4, of the true parameter values, $\rho = 1/3$ and $\phi = 1/4$. For each of these estimates, we plot the corresponding predicted $f(\alpha)$ curves in Figure 7, along with the true $f(\alpha)$ curve.

Observe that the predicted dimensions for low α , positive q , are quite good for all realisations, especially near the information dimension. However, predicted dimensions for high α , negative q , are poor; this is also the case for the Hausdorff dimension which is predicted from the maximum of the $f(\alpha)$ curve.

6 Conclusion

We have presented a method for predicting multi-fractal properties from experimental data. The technique is based on maximising the likelihood that the given finite data set comes from a particular member of a multi-parameter family of well known multi-fractals. The evidence indicates that properties predicted by the proposed method are unbiased by the finite number of sample points in the experimental data.

A valuable feature of the method is that an indication of errors in the best fit parameters is naturally obtained. For example, the indications are that predictions of the generalised dimensions D_q for negative q are extremely unreliable.

Perhaps the method could be improved by increasing the resolution of the correlation density in the $(\log r, \log c)$ plane. However, this would increase the

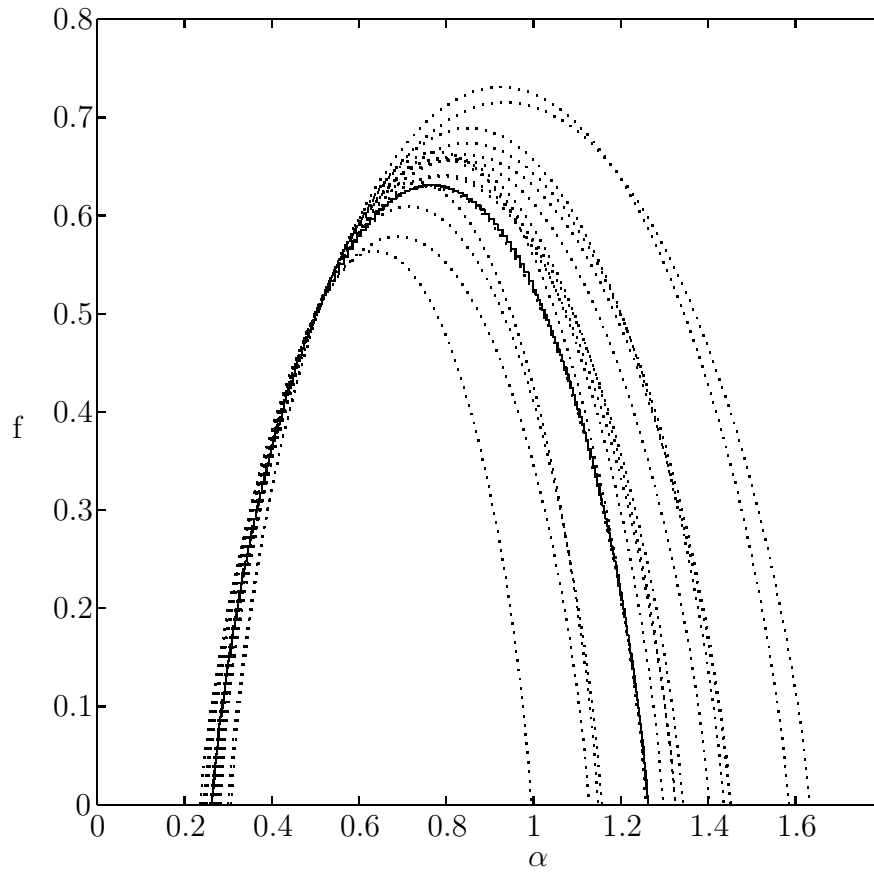


Figure 7: ensemble of multi-fractal spectra $f(\alpha)$, dotted, for each of the predictions plotted in Figure 4 made from samples of $N = 100$ data points. For comparison the multi-fractal spectrum for the actual fractal is plotted as the solid line. Observe the good estimation near the information dimension, but the large errors for larger α .

number of “bins” of low but non-zero density which may reduce the usefulness of the χ^2 test. Furthermore, it will increase the correlations between the counts for each “bin” which may will reduce the quality of the statistics, though perhaps not significantly.

Here we have addressed perhaps the simplest nontrivial example of the process. Most interesting data on spatial fractal distributions lie in two or three dimensions where more complex families of multiplicative multi-fractals need to be employed to model the characteristics of the data distribution. Here we only considered data in one dimension, but even then we should propose a more adaptable approach by modelling the data through, for example, a family of ternary or quaternary multiplicative multi-fractals. for example, such an enlarged family of comparison multi-fractals will enable the method to match multi-fractals with asymmetric $f(\alpha)$ curves.

Furthermore, here we knew the overall size of the fractal and that there is no cut-off at small scales, or indeed that there is no multi-scaling, in the data. The technique will have to be developed further to adapt to these features.

References

- [1] S. Borgani, G. Murante, A. Provenzale, and R. Valdarnini. Multifractal analysis of the galaxy distribution: reliability of results from finite data sets. *Phys Rev E*, 47:3879–3888, 1993.
- [2] L.M. Emmerson and A.J. Roberts. Fractal and multi-fractal patterns of seaweed settlement. preprint, 1995.
- [3] J. Feder. *Fractals*. Plenum Press, 1988.
- [4] P. Grassberger. Finite sample corrections to entropy and dimension estimates. *Phys Lett A*, 128:369–373, 1988.
- [5] T.C. Halsey, M.H. Jensen, L.P. Kadanoff, I. Procaccia, and B.I. Shraiman. Fractal measures and their singularities: the characterization of strange sets. *Phys Rev A*, 33:1141–1151, 1986.
- [6] K. Judd and A. I. Mees. Estimating dimensions with confidence. Technical report, University of Western Australia, 1991.

- [7] B. B. Mandelbrot. Fractals: Form chance and dimension. *J. Fluid Mech.*, 92:206–208, 1979.
- [8] V.J. Martinez. Fractal aspects of galaxy clustering. In Heck and Perdang, editors, *Applying fractals in astronomy*, Lect Notes in Phys m3. Springer-Verlag, 1991.
- [9] G. Paladin and A. Vulpiani. Anomalous scaling laws in multifractal objects. *Phys Rep*, 156:148–225, 1987.
- [10] W.H. press, S.A. Teukolsky, W.T. Vetterling, and B.P. Flannery. *Numerical recipes in FORTRAN. The art of scientific computing*. CUP, 2nd edition, 1992.
- [11] I. Procaccia. Universal properties of dynamically complex systems:the organisation of chaos. *Nature*, 333:618–623, 1988. 16th June.
- [12] K.R. Sreenivasan. Fractals and multifractals in fluid turbulence. *Annu. Rev. Fluid Mech.*, 23:539–600, 1991.